Article

Not peer-reviewed version

Investigation of Pullout Capacity Characteristics of Suction Anchors Under Inclined Loads in Layered Soil

Cheng-Liang Ji , Xia-Tao Zhang , Hao-Yu Wang , Le-Le Liu * , Deng-Feng Fu

Posted Date: 31 October 2025

doi: 10.20944/preprints202510.2499.v1

Keywords: suction anchor; layered soil; inclined loading; finite element; pullout capacity

 doi:10.20944/preprints202510.2499.v1

Article

Investigation of Pullout Capacity Characteristics of Suction Anchors Under Inclined Loads in Layered Soil

Cheng-Liang Ji [1], Xia-Tao Zhang [1], Hao-Yu Wang [2], Le-Le Liu [2,*] and Deng-Feng Fu [2]

[1] Shandong Electric Power Engineering Consulting Institute Corporation Limited, Jinan 250013, China

[2] Shandong Engineering Research Center of Marine Exploration and Conservation, Ocean University of China, Qingdao 266100, China

* Correspondence: lele.liu@ouc.edu.cn; Tel.: +86-18561710610

Abstract

Suction anchors are widely used in marine engineering because of its easy installation, cost-effectiveness, and excellent load-bearing capacity. However, existing research on its bearing capacity has primarily focused on homogeneous soils, which fails to adequately reflect the actual bearing capacity of layered seabed soils. Therefore, this study conducted a series of numerical simulations to investigate the pullout bearing capacity of suction anchors subjected to inclined loads in upper- stiff-lower-soft layered clay. By considering the clay strength (S_{um}/kD) and soil layer thickness ratio (T_h/L, T_c/L), this study systematically explores influence on the optimal centerline loading depth ($Z_{cl,opt}$), uniaxial ultimate bearing capacity (H_{ult} and V_{ult}), and the VH failure envelope of suction anchors. The results indicate that the layer thickness ratio T_h/L of lightly overconsolidated clay (LOC) is the key factor influencing the $Z_{cl,opt}$ and ultimate bearing capacity H_{ult} and V_{ult}. An increase in T_h/L significantly enhances the pullout resistance of suction anchors, which primarily results from the combined enhancement effect of lateral friction resistance and end resistance at the anchor-soil interface. The layered clay has a distinct influence on the horizontal and vertical bearing capacities of suction anchors. Based on the results of parameter analysis, a conservative analytical expression for the lower bound of the VH failure envelope curve is further proposed. The research conclusions provide theoretical basis and engineering practice guidance for the optimized design and safety assessment of suction anchors in layered soil.

Keywords: suction anchor; layered soil; inclined loading; finite element; pullout capacity

1. Introduction

Suction anchors typically refer to cylindrical structures that are closed at the top and open at the bottom, commonly constructed of steel or concrete [1,2]. Its diameter is typically 3–7 meters, with wall thickness ranging from 25 to 75 millimeters, and the L/D is typically between 1 and 10 [3].Suction anchors are widely used in coastal floating platforms, offshore wind turbine foundations, and deepwater projects due to their rapid installation, low cost, high load-bearing capacity, and minimal disturbance to seabed soil layers [4,5]. During the installation of suction anchors, the anchors are initially driven into the seabed soil using their own weight. Subsequently, water is pumped out through the suction holes at the top of the anchor, which creates a pressure differential between the interior and exterior of the anchor. This pressure differential forces the anchor to continue driving into the soil. When the top cover of the suction anchor makes contact with the seabed soil, the anchor is considered fully penetrated [6,7].

In actual engineering environments, offshore structures inevitably experience the effects of waves, wind, and currents [8,9]. Since the load must be transmitted to the suction anchor via the suspension chain and mooring chain, the suction anchor is continuously subjected to inclined loads

 doi:10.20944/preprints202510.2499.v1

[10]. The bearing mechanism of suction anchors subjected to inclined pullout loads differs from that of suction anchor foundations bearing vertical loads at the top. The loading angle and padeye location alter the failure mode of suction anchors [11]. Keaveny et al. [12]conducted prototype tests on a series of suction anchors installed in clay, and applied mooring forces to the padeyes of the anchors below the mud surface. The test results indicate that when the mooring force is applied at the midpoint below the mud surface of the suction anchor, the corresponding ultimate bearing capacity is twice that when applied at the mud surface. Newlin [13] studied that when mooring forces are applied below the optimal padeye position, the top of the suction anchor tilts away from the mooring force direction upon failure. In this case, the failure mode is not pullout failure but rotation within the soil. The suction anchor can obtain its maximum bearing capacity only when the anchor undergoes translational displacement. Therefore, the loading angle and padeye are critical factors affecting suction anchors.

To explore the ultimate bearing capacity of suction anchors under inclined loads, numerous studies have been conducted through theoretical analysis, numerical simulation, and physical testing. Current research primarily focuses on suction anchors in homogeneous soil. Wang et al. [14] conducted load-controlled model tests on the ultimate bearing capacity of suction anchors in soft clay, and analyzed the effects of loading direction on failure modes and ultimate bearing capacity. The test results indicate that the bearing capacity of suction anchors is influenced by the loading direction. The reverse bearing capacity of the soil layer below the anchor base is a key factor affecting the ultimate bearing capacity of suction anchors. Zhang et al. [15] investigated the effect of cutting grooves on the ultimate bearing capacity of suction anchors in NC through numerical simulation methods. Kim et al. [16] investigated the behavior of suction anchor foundations installed in cohesionless soil under horizontal loading through numerical simulation. They conducted parametric studies on different length to diameter ratios and padeye position of the suction anchors. The horizontal bearing capacity of the suction anchors was estimated, and soil stress distribution was analyzed under loading applied at the optimal padeye position. Existing studies on the bearing capacity of suction anchors have primarily focused on single homogeneous soil layers, which lack consideration of the actual layered characteristics of soil masses [17,18]. However, under the influence of geological movements and sedimentation processes, the actual seabed typically exhibits natural layering or anisotropic properties along the depth direction. The characteristics of such layered soil differ significantly from those of the current single-layer homogeneous soil layers studies [19,20]. In natural layered soils, a typical layered soil structure occurs where stronger soil layers overlie weaker layers [21]. For example, in the Bohai oil and gas fields off of China, the seabed exhibits a layered structure with upper- stiff-lower-soft layers depending on factors such as estuarine sediment transport patterns and tidal currents [22,23]. Additionally, in areas such as the Gulf of Guinea, the Bass Strait off southeastern Australia, and the Joa oil field in the North Sea, the seabed also contains hard soil layers with significantly greater strength than the underlying soil [24,25]. Furthermore, existing design guidelines for piles in layered soils primarily employ the equivalent lateral friction coefficient of the piles and the p–y curve method for lateral friction resistance. This approach is unsuitable for predicting the pullout resistance of suction anchors in layered soils. Existing guidelines, such as those from the American Petroleum Institute (API) [26] and DNV [27], typically assume homogeneous and uniform soil properties. Applying these existing guidelines to predict bearing capacity under layered soil conditions may be overly conservative. Therefore, it is important to fully consider the influence of layered soil properties to gain a deeper understanding of the pullout resistance capacity of suction anchors.

Based on the above-mentioned research status, this study aims to investigate the ultimate bearing capacity of suction anchors in upper- stiff-lower-soft layered clay. To analyze the bearing capacity of suction anchors under inclined loads, numerical simulation methods were employed. Considering variations in clay strength (S_{um}/kD) and layer thickness ratios (T_h/L、T_c/L、T_n/L), the ultimate bearing capacity of suction anchors subjected to inclined loads in layered clay (lightly overconsolidated clay (LOC), normally consolidated clay (NC), low-strength normally consolidated

 doi:10.20944/preprints202510.2499.v1

clay (LNC)) was investigated. The primary research content includes: (1) Determined the optimal centerline loading depth $Z_{cl,\ opt}$ in layered clay; (2) Obtained the corresponding uniaxial ultimate bearing capacities H_{ult} and V_{ult}; (3) Quantified the suction anchor VH failure envelope under inclined loading and derived an analytical expression for its lower bound solution.

2. Numerical Modeling

2.1. Geometry and Mesh

By referring the studies of Kim et al. [28] and Fu et al. [29], the numerical simulation model selected the suction anchor diameter D=5m, depth of embedment L=7.5m, with L/D=1.5 and thickness t =50mm. The selected suction anchor dimensions are commonly adopted in engineering practice [30,31]. As shown in Figure 1(a), the suction anchor is installed in layered clay. As the stiffness of suction anchors and soil differs significantly, suction anchors are typically treated as rigid bodies to improve computational efficiency. This method is widely applied in offshore geotechnical engineering [28,29,32]. The suction anchor is modeled using rigid materials with a density of $\rho = 6800$ kg/m^3, elastic modulus E = 210 GPa, and Poisson's ratio v = 0.3. An inclined load is applied by setting a reference point on the suction anchor.

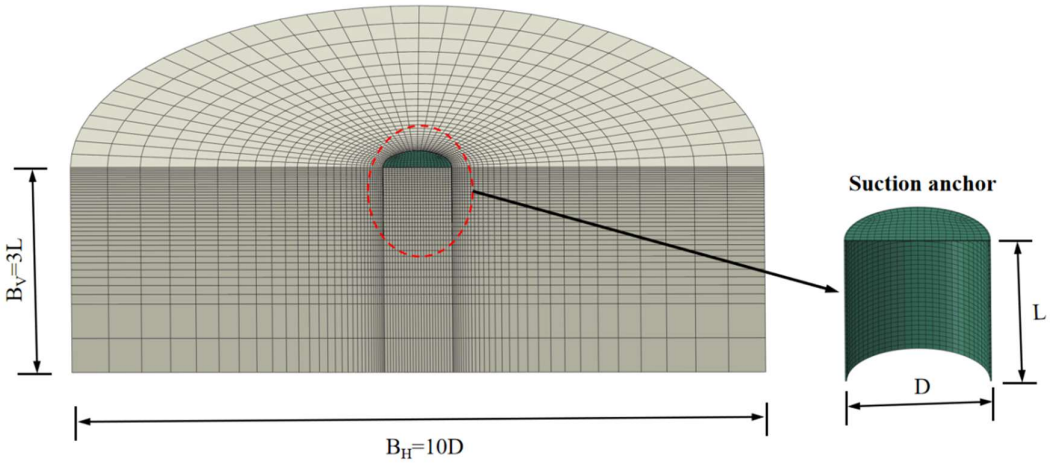

(**a**)

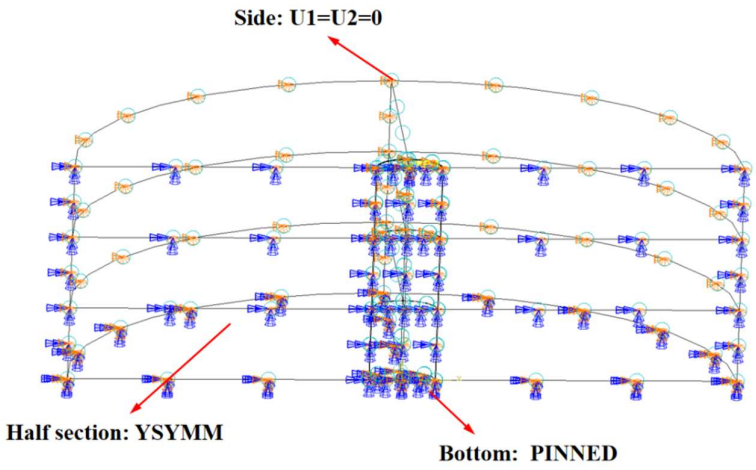

(**b**)

Figure 1. Schematic diagram of the numerical model.

 doi:10.20944/preprints202510.2499.v1

In this study, a three-dimensional finite element model was constructed using the commercial software ABAQUS 2020. The suction anchor and soil mass were modeled using three-dimensional eight-node solid elements (C3D8H). Due to load symmetry, only half of the soil mass was modeled to improve computational efficiency. The minimum mesh size for the model is 0.02D. Based on existing research and sensitivity analysis of mesh sizes, the selected minimum mesh size is reasonable [33,34]. The length and height of the soil are B_H=10D and B_V=3L, respectively, with the suction anchor positioned at the center of the soil model. The model dimensions are selected sufficiently to eliminate the influence of boundary effects [18,35]. The relevant constraints on the soil are shown in Figure 1(b).

2.2. Geometry and Mesh

The clay in this study is treated as an elastoplastic material, adhering to the Tresca yield criterion and associated flow rules. The Poisson's ratio of the clay is v=0.49, which is used to simulate undrained conditions where volume remains constant. The undrained shear strength of the clay is satisfied:

$$S_u = S_{um} + kz \tag{1}$$

Where, S_{um} represents the undrained shear strength of the soil at the mud surface, k represents the gradient of clay strength with depth, and z represents the depth below the mud surface. The soil elastic modulus is taken as E=500S_u, and the normalized parameter S_{um}/kD is used to evaluate the influence of soil properties on bearing capacity. Referencing relevant studies and geological exploration reports, S_{um}/kD = 0, 0.4, 0.67, 1.0 [36–39], the relevant parameters of the clay are shown in Table 1. The numerical simulation tests for suction anchors are outlined in Table 2.

Table 1. Clay parameters.

Parameter	Clay A	Clay B	Clay C	Clay D
S_{um} (kPa)	0.1	3	5	10
k（kPa/m）	1.25	1.5	1.5	2
γ′（kN/m3）	6	6	6	7.2
S_{um}/kD	0	0.4	0.67	1

Table 2. The experimental setup for the suction anchor numerical simulation test.

Group	S_{um}/kD (T_h)	S_{um}/kD (T_c)	T_h/L	T_c/L	T_n/L	
Group A	—	—	—	—	—	Model validation
Group B	1	0.4、0.67、1	0.5、0.75、1.25	0.5、0.75、1.25		To determine the optimum centerline loading depth $Z_{cl,opt}$
Group C	1	0.4、0.67、1	0.5、0.75、1.25	0.5、0.75、1.25	(3L-T_h-T_c)/L	To calculate the uniaxial ultimate bearing capacity (H_{ult} and V_{ult})
Group D	1	0.4、0.67、1	0.5、0.75、1.25	0.5、0.75、1.25		To calculate the VH failure envelopes

To investigate the bearing capacity of suction anchors in upper- stiff-lower-soft layered clay under inclined loading, the soil in this study was divided into three layers. The first layer consists of LOC with S_{um}/kD=1.0, and layer thickness ratios T_h/L=0.5, 0.75 and 1.25. The second layer comprised

 doi:10.20944/preprints202510.2499.v1

either NC or LOC, with S_{um}/kD values of 0.4, 0.67, and 1.0, and layer thickness ratios T_c/L =0.5, 0.75 and 1.25. The third layer consists of LNC, with S_{um}/kD = 0, and a soil layer thickness ratio T_n/L=(3L-T_h-T_c)/L. The relevant parameters were obtained by referring to related research and geological exploration reports. Regarding the bearing capacity of suction anchors in clay, due to the low permeability coefficient of clay, numerous studies have assumed the soil as undrained conditions[34,40–42].

2.3. Details of Analysis and Loading Methods

The finite element modeling process consists of three steps:

(1) The initial geostress equilibrium stage: This section performs geostress equilibrium analysis of the soil mass only, and the suction anchor is treated as void space. In the initial geostress equilibrium stage, the anchor-soil interface contact is not activated.

(2) The contact activation stage: After the soil stress equilibrium is established, the anchor-soil interface contact is activated. This means the penetration process of the suction anchor is disregarded, and the suction anchor is considered to be in the "in-place" state.

(3) The load application stage: A reference point RP is established at the suction anchor to apply the inclined load. The inclined pull-out load is applied under displacement control, with a maximum allowable displacement of 0.2D. The selection of the maximum displacement references the research by Supachawarote[32].

The tangent method was employed to determine the uniaxial bearing load capacity, by referring to the study of Long et al. [43], for which no distinct yield value was observed when the load-displacement curve reached its maximum displacement. When the suction anchor moves horizontally or vertically without rotation, the uniaxial bearing capacity is equivalent to the uniaxial ultimate bearing capacity H_{ult} and V_{ult}. The complete VH failure envelopes for the suction anchor can be obtained through sweep analysis, reverse sweep analysis, and probe analysis, which has been widely applied[32].

As shown in Figure 2, when the suction anchor moves horizontally under inclined loading without rotation, the inclined load can be simplified into a horizontal force H, a vertical force V, and a constraining moment M. By applying the principle of moment equilibrium, the optimal padeye depth $Z_{pad,opt}$ at the corresponding angle and the optimal centerline loading depth $Z_{cl,opt}$ can be obtained, which satisfy the equation:

$$Z_{cl,opt} = \frac{M}{H} \tag{2}$$

$$Z_{cl,opt} = Z_{pad,opt} + \frac{D}{2} \times \tan\theta \tag{3}$$

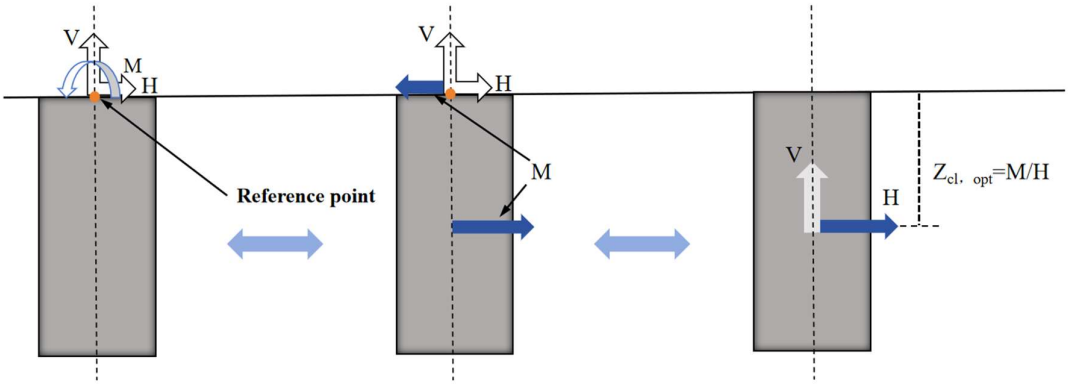

Figure 2. The schematic diagram of the optimum centerline loading depth for the suction anchor.

 doi:10.20944/preprints202510.2499.v1

3. Model Validation

To validate the accuracy of the constructed numerical model, the numerical simulation results of suction anchors under inclined loading were compared with existing experimental results, as shown in Figure 3. It can be seen from Figure 3 (a), for NC with S_u=1.25z and L/D=1.5, the numerical simulation results show excellent consistency with test results from Supachawarote [32] and experimental results from the Norwegian Geotechnical Institute (NGI), Offshore Technology Research Center (OTRC), and Center for Offshore Foundation Systems (COFS). The VH envelope obtained from the numerical model closely matches their findings, which indicates that the numerical model developed in this study can effectively reproduce the pullout behavior of suction anchors in clay.

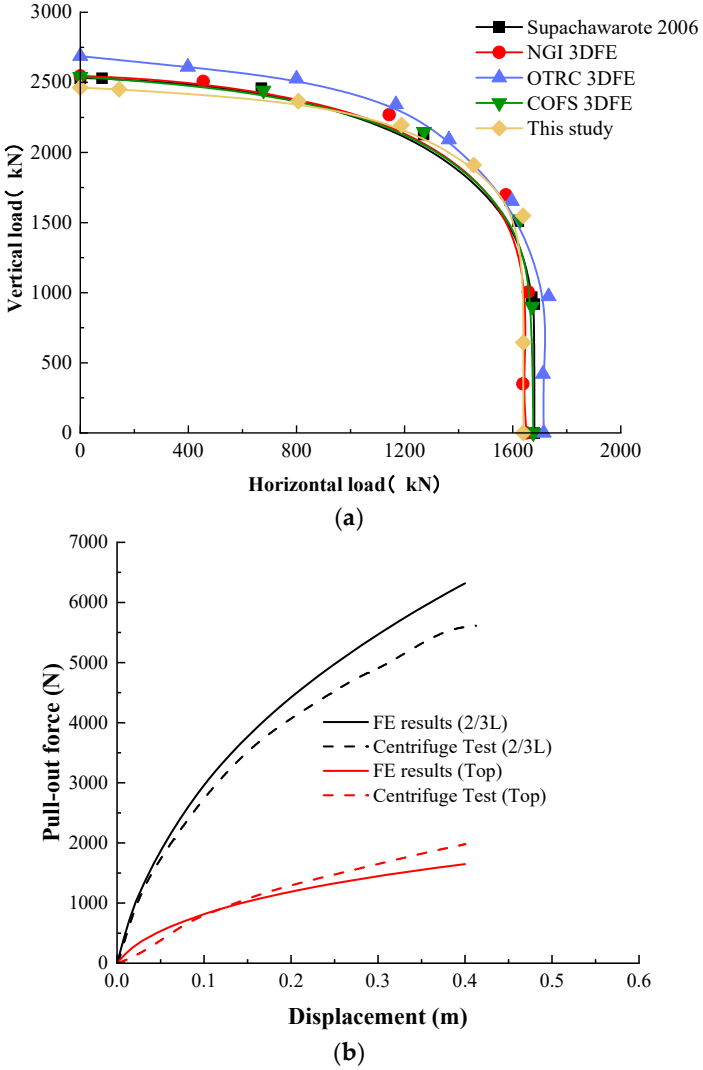

Figure 3. Model validation.

Furthermore, the accuracy of the constructed numerical simulation model was further validated by referencing centrifuge test data and finite element modeling results for non-cohesive soils from Kim et al. [17,28].The Loads were applied at the top of the suction anchor and below the mud surface at Z_{pad}=2/3L, with cu=7 kPa, internal friction angle φ=32°, and dilation angle ψ=8°. The selection of relevant parameters strictly followed those used in the centrifuge tests and finite element model. The corresponding comparison results are shown in Figure 3(b), which shows that the constructed numerical model can effectively characterize the bearing capacity of the suction anchor.

 doi:10.20944/preprints202510.2499.v1

4. Results of Numerical Analyses

4.1. Optimum Centerline Loading Depth $Z_{cl,\ opt}$

The optimal centerline loading depth $Z_{cl,opt}$ is the key factor determining whether the suction anchor undergoes translational or rotational motion under inclined loading. When the inclined load vector applied to the suction anchors padeye passes through $Z_{cl,opt}$, the suction anchors move horizontally under the inclined load without rotation. At this point, the inclined load corresponds to the maximum pullout force at the given mooring angle. When the inclined load vector applied to the anchor padeye deviates from $Z_{cl,opt}$, the suction anchor will rotate forward or backward during the pullout process, correspondingly reducing the pullout resistance of the suction anchor. Therefore, $Z_{cl,opt}$ is an indicator reflecting the pullout resistance capacity and failure mode of the suction anchor under corresponding soil parameter conditions. In engineering design, the location of $Z_{cl,opt}$ must be prioritized for determination.

Figure 4 shows the influence of different soil mechanical parameters and layer thickness on the optimal centerline loading depth $Z_{cl,opt}$ for layered clay. It can be seen that the LOC thickness ratio T_h/L is the key factor controlling $Z_{cl,opt}$. Taking $S_{um}/kD = 0.4$ as an example, when $T_h/L = 0.5$, half of the suction anchor is embedded in the LOC layer, with $Z_{cl,opt} = 0.65$. With the increase in T_h/L to 0.75 and 1.25, the upper portion of the suction anchor contributes more lateral friction resistance due to the increased thickness of the LOC layer. To balance the moments, the suction anchors $Z_{cl,opt}$ shift downward, with corresponding $Z_{cl,opt}$ being 0.67 and 0.71, respectively. When $T_h/L > 1$, the suction anchor is fully embedded in the LOC layer. The values of $Z_{cl,opt}$ remain nearly unchanged for different S_{um}/kD and T_c/L, as the high strength of the LOC soil dominates the pullout resistance. When $T_h/L = 0.5$ and $T_c/L = 0.5$, the suction anchor end is located between the NC layer and the LNC layer interface. It can be observed that the variation of $Z_{cl,opt}$ at this point is still influenced by the higher-strength clay within the suction anchor, which means that the impact of high-strength clay on $Z_{cl,opt}$ is significantly greater than that of low-strength clay.

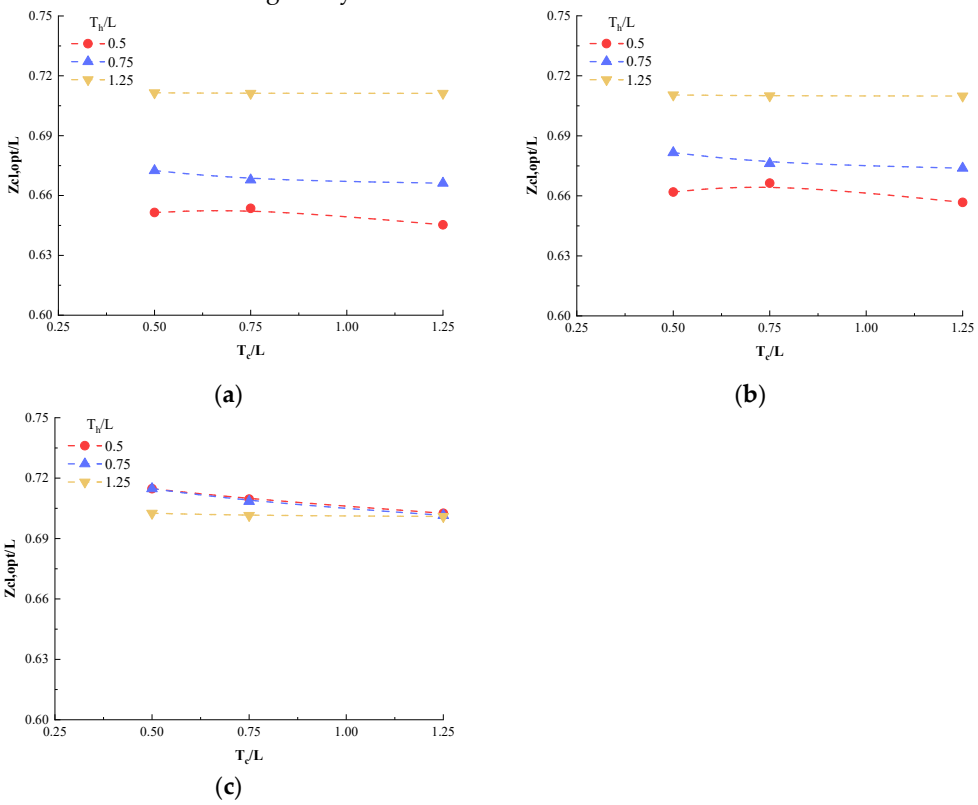

Figure 4. The effect of layered soil thickness on the optimal centerline loading depth $Z_{cl,opt}$.

 doi:10.20944/preprints202510.2499.v1

4.2. Uniaxial Ultimate Bearing Capacity (H_{ult} and V_{ult})

The uniaxial ultimate bearing capacity (H_{ult} and V_{ult}) represents the pullout resistance of the suction anchors when subjected to horizontal or vertical pullout forces without rotation. In numerical simulations, the uniaxial ultimate bearing capacity equals the integral of the ultimate lateral friction resistance along the anchorage depth. Based on the above principles, the effects of suction anchor relative positions (T_h/L and T_c/L) and soil strength (S_{um}/kD) on uniaxial ultimate bearing capacity were quantified. The uniaxial ultimate bearing capacities H_{ult} and V_{ult} of suction anchors under different conditions are shown in Tables 3-5.

As shown in Tables 3-5, the LOC thickness ratio T_h/L is the core factor determining the uniaxial ultimate bearing capacity. Specifically, the undrained shear strength of LOC is significantly higher than that of NC and LNC. As the embedment length of the suction anchor into the LOC increases, the combined effect of lateral friction resistance and end resistance at the anchor-soil interface becomes more pronounced. Taking S_{um}/kD = 0.67 and T_c/L = 0.5 as examples, when T_h/L increases from 0.5 to 1.25, the corresponding horizontal ultimate bearing capacity H_{ult} of the suction anchor rises from 4182.01 kN to 5096.61 kN, representing an increase of approximately 21.9%. The vertical ultimate bearing capacity V_{ult} increases from 4457.01 kN to 6566.56 kN, representing an increase of approximately 47.3%. This supports the findings of Zhou et al. [18,43], which concluded that the pullout resistance of suction anchors in layered soils is positively correlated with the thickness of the anchor embedded in the higher undrained strength clay layer. As the anchor embedment depth in the higher undrained strength clay layer increases, both lateral friction resistance and end resistance enhance during anchor-soil interface interaction under pullout forces.

The corresponding displacement contour map (Figure 5) also shows that as T_h/L increases from 0.5 to 1.25, the suction anchors experience passive earth pressure on the external wall under horizontal loading, which results in the formation of a passive earth pressure zone. The extent of this passive earth pressure zone is primarily influenced by the length L of the suction anchor. When the suction anchor length remains constant, the horizontal ultimate bearing capacity is primarily influenced by the strength of the clay surrounding the anchor.

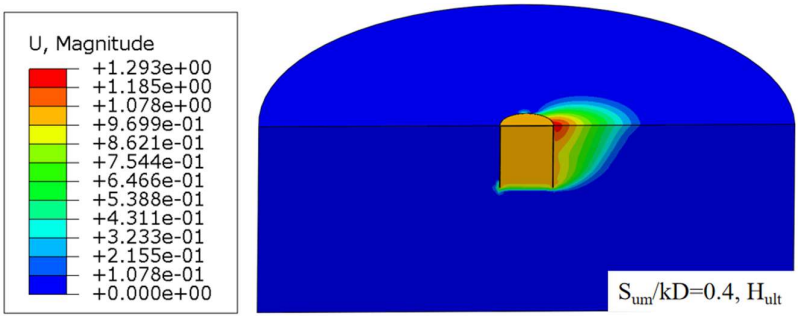

(**a**)

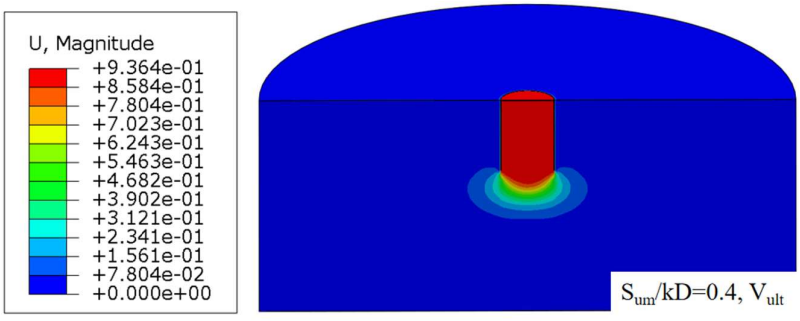

(**b**)

 doi:10.20944/preprints202510.2499.v1

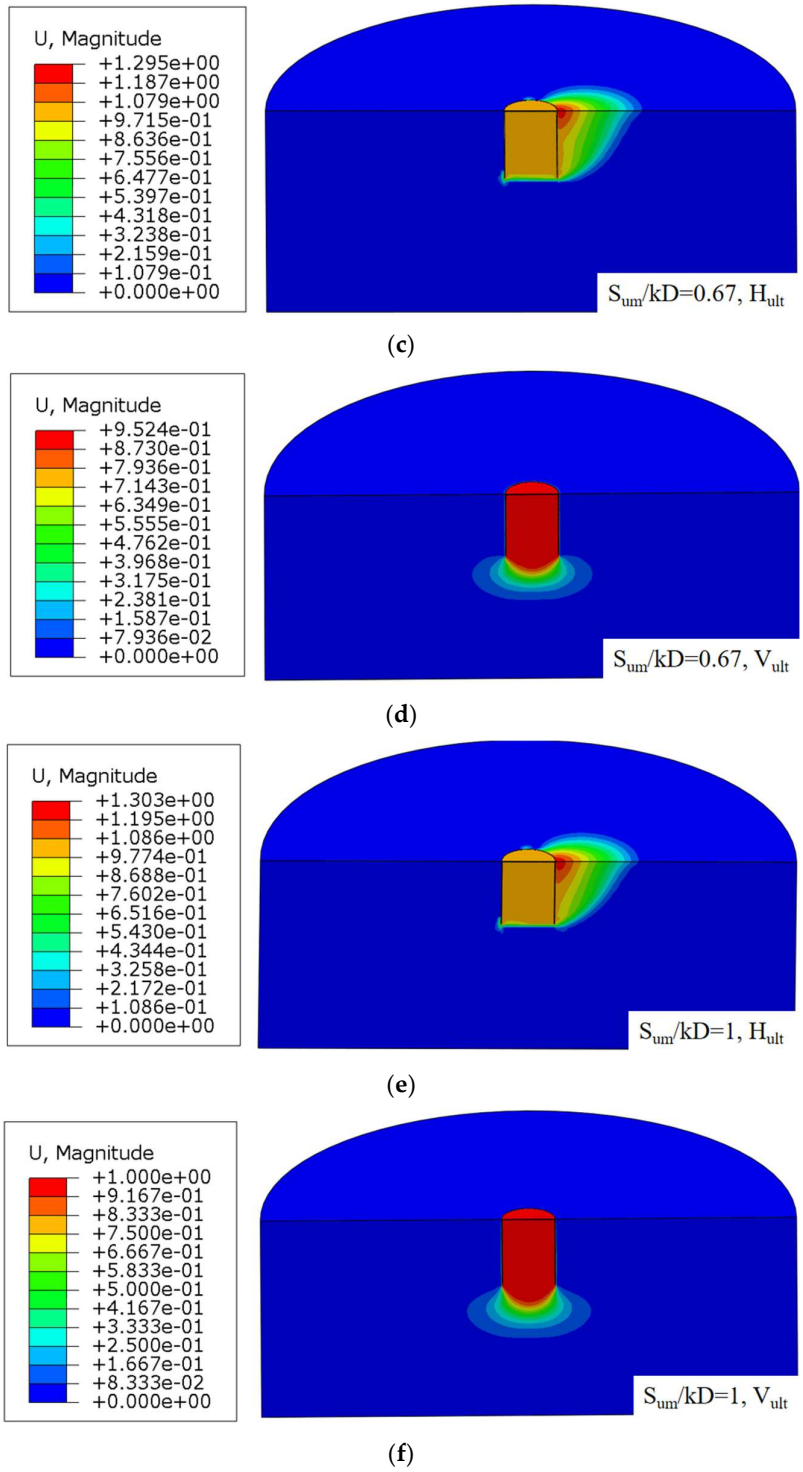

Figure 5. The displacement contour plots of suction anchors under horizontal/vertical loads (S_{um}/kD =0.67, T_c/L=0.5): (a-b) T_h/L=0.5; (c-d) T_h/L=0.75; (e-f) T_h/L=1.25.

When subjected to vertical loads, the pullout resistance of suction anchors is primarily composed of the anchor-soil lateral friction resistance and end resistance. With the increase in the thickness ratio T_h/L of the LOC soil layer, Figure 5 shows that the end resistance influence zone expands. This means the contribution of end resistance to the vertical bearing capacity of the suction anchor increases, and consequently, the corresponding vertical ultimate bearing capacity V_{ult} increases. The vertical ultimate bearing capacity is primarily influenced by the thickness ratios T_h/L and T_c/L.

 doi:10.20944/preprints202510.2499.v1

The layered clay makes the soil strength along the clay surface exhibit non-uniformity. The increase in S_{um}/kD enhances the uniaxial bearing capacity of layered clay. Taking $T_h/L=0.5$ and $T_c/L=0.5$ as examples, when S_{um}/kD increases from 0.4 to 1.0, H_{ult} rises from 3990.1 kN to 5017.5 kN, an increase of approximately 25.7%; V_{ult} increases from 4195.2 kN to 5341.32 kN, an increase of approximately 27.3%. The higher the S_{um}/kD , the greater the overall shear strength of the layered soil, and both the friction resistance and end resistance at the anchor-soil interface will increase simultaneously. The soil strength S_{um}/kD is positively correlated with bearing capacity; the higher the soil strength, the greater the corresponding bearing resistance. The thickness of the LNC soil layer has no significant effect on H_{ult} and V_{ult}. The displacement vector contour plots for layered soil subjected to horizontal/vertical loads are shown in Figure 6.

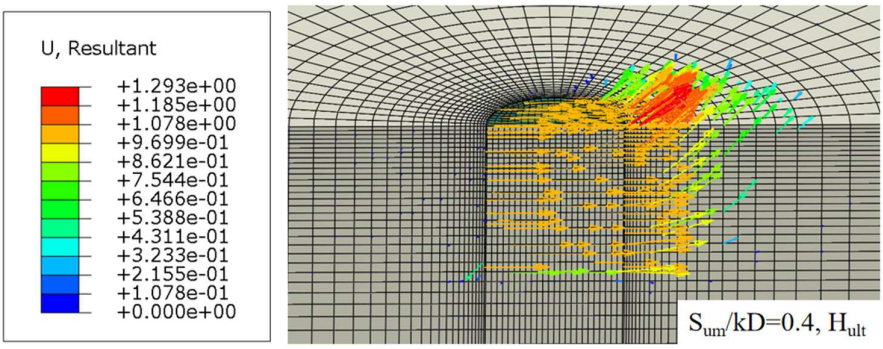

(**a**)

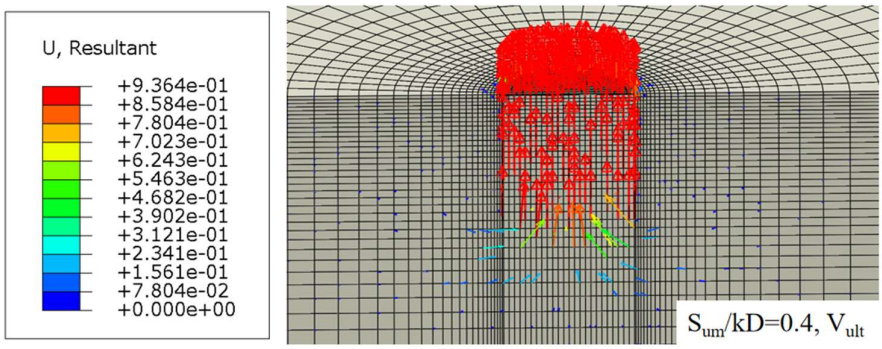

(**b**)

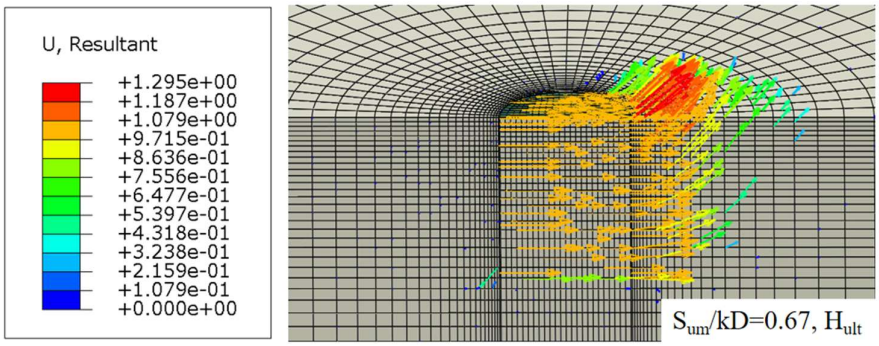

(**c**)

 doi:10.20944/preprints202510.2499.v1

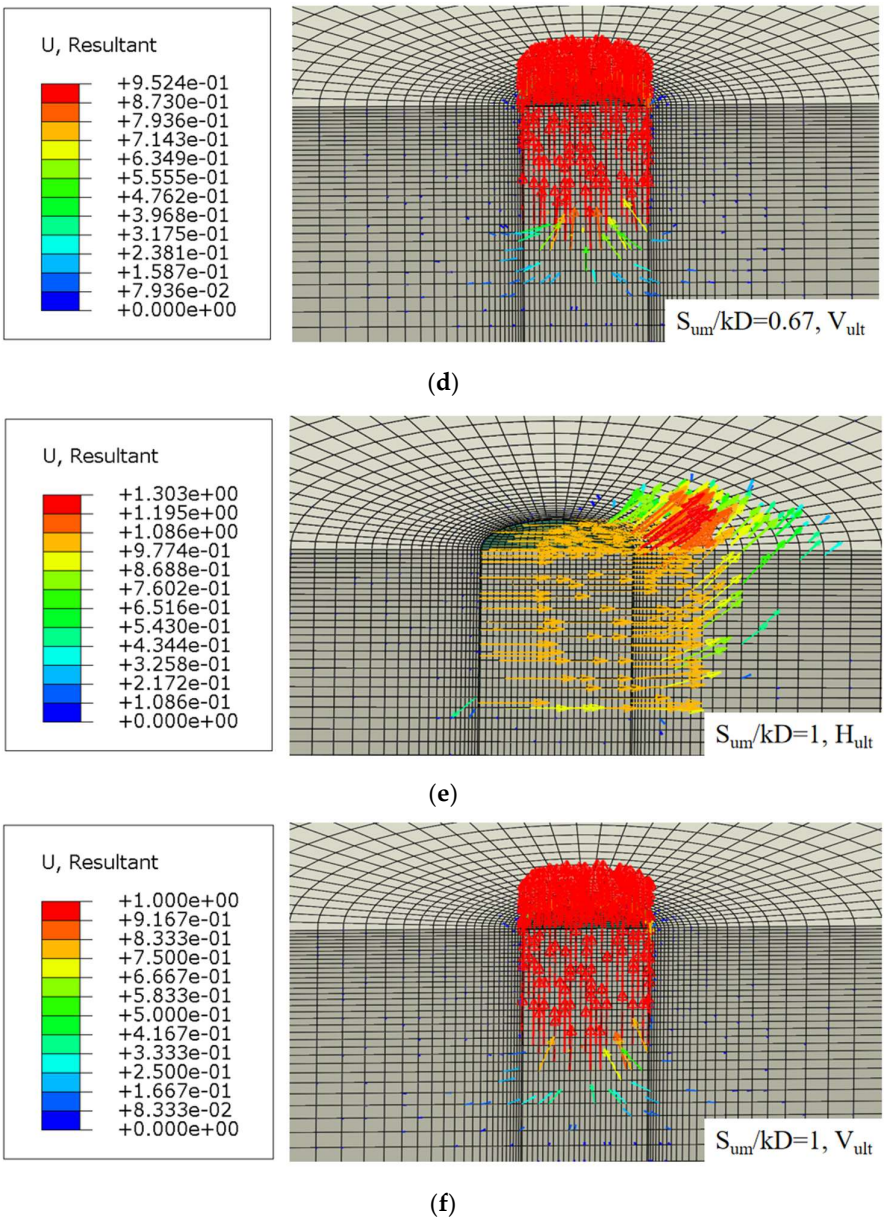

Figure 6. The displacement vector plots of suction anchors under horizontal/vertical loads (T_h/L, T_c/L=0.5): (a-b) S_{um}/kD =0.4; (c-d) S_{um}/kD =0.67; (e-f) S_{um}/kD =1.

It can be observed that when the thickness ratios T_h/L and T_c/L remain unchanged, the corresponding horizontal/vertical load-displacement vector plots show little variation. This indicates that at this point, the bearing capacity of the suction anchor is primarily influenced by the friction resistance at the anchor-soil interface.

The thickness ratio T_c/L of the NC soil layer has little effect on the horizontal ultimate bearing capacity H_{ult} but significantly affects the vertical ultimate bearing capacity V_{ult}. For example, when S_{um}/kD=1.0 and T_h/L=0.5, as T_c/L increases from 0.5 to 1.25, H_{ult} changes little, rising only from 5017.5 kN to 5085.19 kN. Meanwhile, V_{ult} increases from 5341.32 kN to 7211.5 kN, representing an increase of approximately 35.0%. Combining Figure 5 and 6 with the studies by Supachawarote [32]: Vertical bearing capacity relies more on the accumulated effect of friction resistance at the anchor-soil interface. As the strength of the clay in the suction anchorage zone increases, the friction resistance becomes more pronounced. In contrast, horizontal bearing capacity is dominated by the distribution

 doi:10.20944/preprints202510.2499.v1

pattern of lateral resistance. The influence of T_c/L on H_{ult} is smaller than that of T_h/L and S_{um}/kD, which leads to a relatively minor overall change in H_{ult}.

When $T_h/L > 1$, which corresponded to the suction anchor being fully embedded in the LOC layer, the horizontal ultimate bearing capacity H_{ult} tended toward stability. Meanwhile, the vertical ultimate bearing capacity V_{ult} still shows a slight increase, which reflects that the vertical bearing capacity is more complex affected by the coupling of multiple soil layers. The lower soil layers (NC, LNC) still contribute to the end resistance.

4.3. The VH Failure Envelopes

The VH failure envelopes for layered soil are shown in Figure 7. By dimensionless processing of horizontal and vertical bearing capacities using $H_0/\gamma'D$ and $V_0/\gamma'D$, respectively, the effects of parameters such as suction anchor dimensions and soil weight are eliminated.

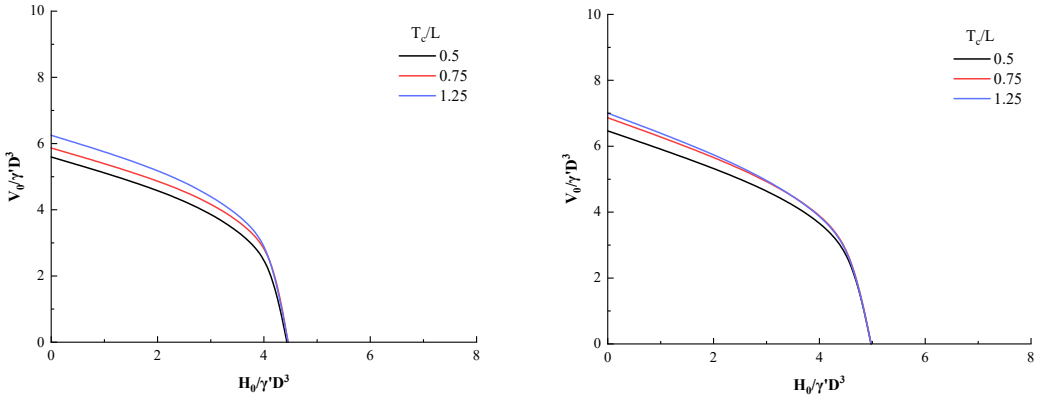

(**a**)T_h/L=0.5, S_{um}/kD =0.4 (**b**)T_h/L=0.75, S_{um}/kD =0.4

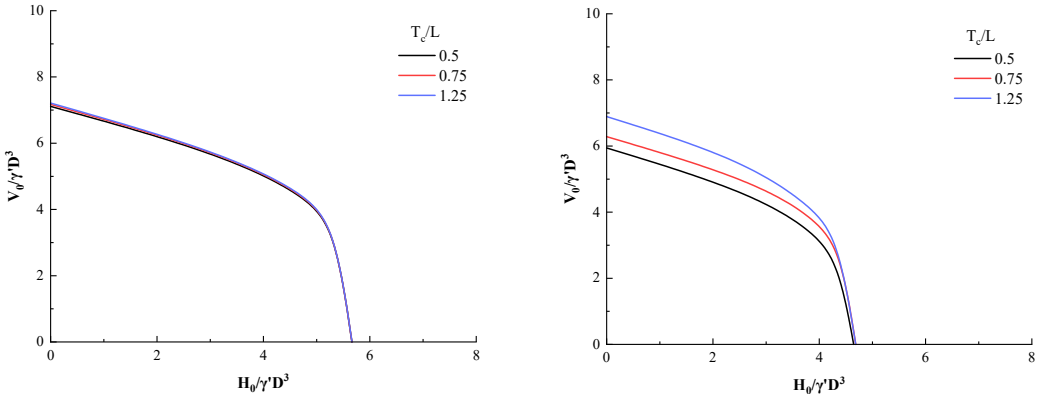

(**c**)T_h/L=1.25, S_{um}/kD =0.4 (**d**)T_h/L=0.5, S_{um}/kD =0.67

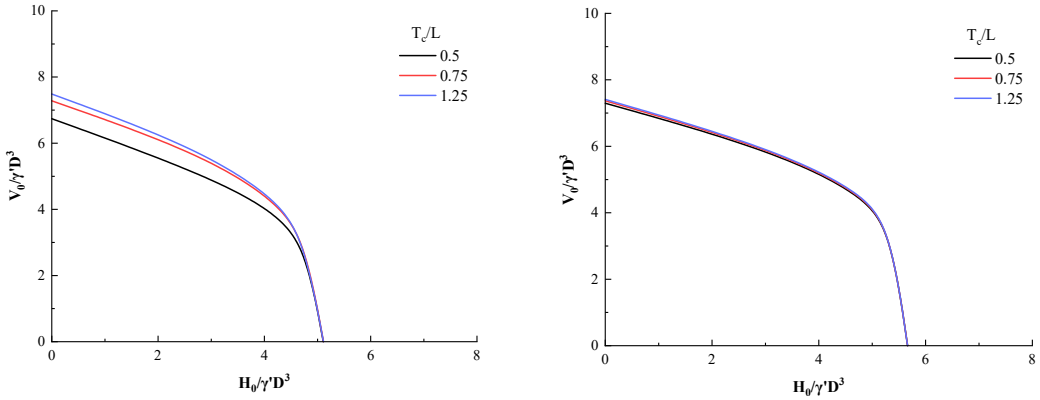

(**e**)T_h/L=0.75, S_{um}/kD =0.67 (**f**)T_h/L=1.25, S_{um}/kD =0.67

 doi:10.20944/preprints202510.2499.v1

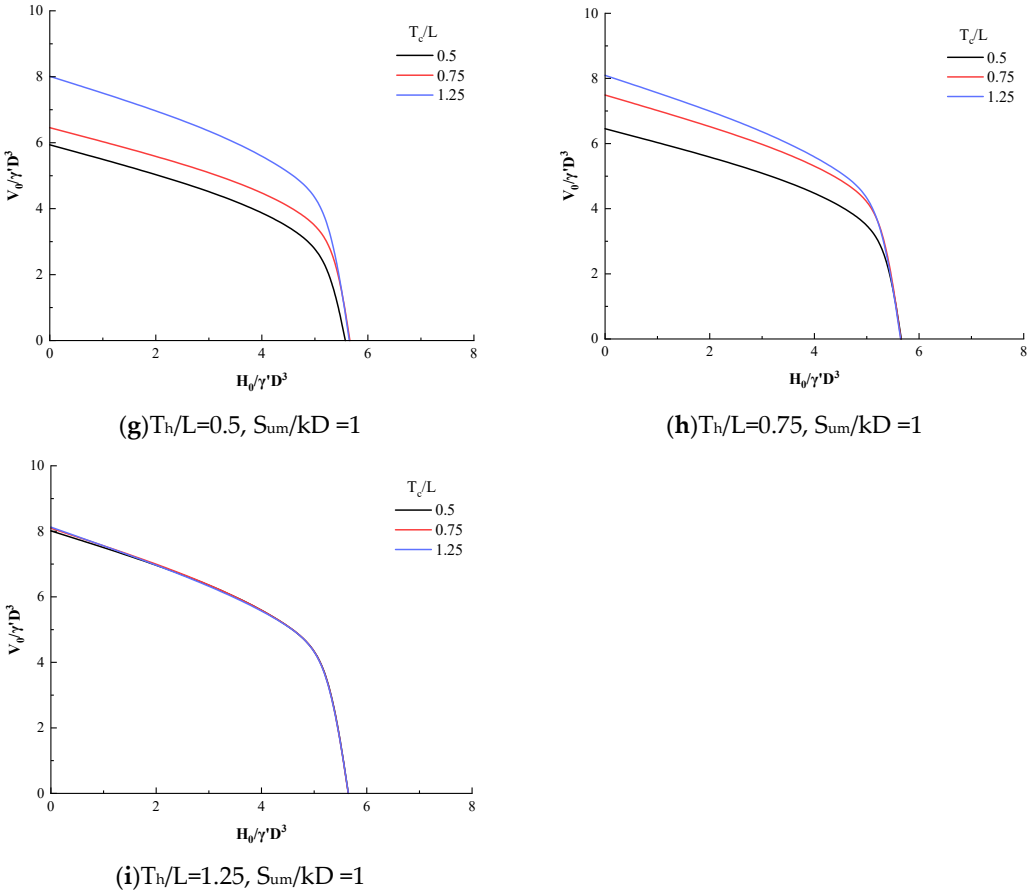

(**g**)T_h/L=0.5, S_{um}/kD =1 (**h**)T_h/L=0.75, S_{um}/kD =1

(**i**)T_h/L=1.25, S_{um}/kD =1

Figure 7. The VH failure envelopes.

As shown in Figure 7, with the increase in the LOC layer thickness ratio T_h/L (from 0.5 to 1.25), the horizontal bearing capacity of the VH failure envelopes significantly increases under the same vertical load. This indicates that the total area of the VH failure envelopes expands, which means the corresponding combined uniaxial bearing capacity improves. The LOC soil layer exhibits relatively high strength. As the thickness ratio T_h/L increases, the contact area between the suction anchor and the high-strength clay expands. This allows the anchor-soil interface to provide more uniform and substantial lateral friction resistance. Consequently, when horizontal loads increase, the attenuation of vertical loads becomes more gradual. The research findings align with the conclusions of Zhao et al. [44], indicating that the embedment length of suction anchors in high-strength soil layers is positively correlated with the combined bearing capacity.

The VH failure envelopes in layered clay exhibit asymmetry, which indicates that layered clay has a distinct influence on the horizontal and vertical bearing capacities of suction anchors. The horizontal friction resistance of the suction anchors dominates when horizontal loads dominate, with the thickness of the LOC layer determining the horizontal bearing capacity. When vertical loads dominate, the friction resistance at the anchor-soil interface and the end resistance play key roles, while the vertical bearing capacity is influenced by both the LOC and the underlying NC and LNC layers.

To visually represent the relative shape of the VH failure envelope, the results can be normalized based on the uniaxial bearing capacity H_0 and V_0. Extensive research indicates that the only lower bound solution of the VH failure envelope can be observed through relevant processing, which shows that the normalized VH failure envelope is independent of soil layer thickness and soil properties[45,46]. This conservative solution method allows the yield envelope in the VH envelope

 doi:10.20944/preprints202510.2499.v1

to be obtained simply by scaling H_0 and V_0. Based on previous research findings and regression analysis, the lower bound of the VH failure envelope, as shown in Figure 8, and can be expressed as:

$$\frac{H_0}{H_{ult}} = \left\{1 - \left(\frac{V_0}{V_{ult}}\right)^3\right\}^{1/0.85} \tag{4}$$

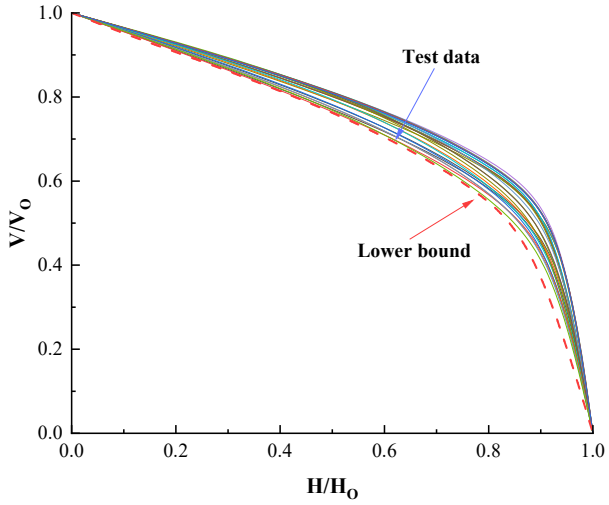

Figure 8. The normalized VH failure envelope.

Where, $\frac{V_0}{V_{ult}}$ represents the normalized vertical bearing capacity; $\frac{H_0}{H_{ult}}$ represents the normalized horizontal bearing capacity. The exponent 1/0.85 indicates that vertical bearing capacity reduces the capacity of horizontal bearing capacity. Meanwhile, the ultimate bearing capacity of suction anchors installed in layered clay can be obtained by multiplying the corresponding ultimate bearing capacities H_{ult} and V_{ult} by Equation (4).

5. Discussion

In this paper, the bearing capacity of suction anchors subjected to inclined loads in upper- stiff-lower-soft layered clay is systematically investigated. Numerical simulation results indicate that the clay strength S_{um}/kD and the thickness ratio T/L are the core factors determining the bearing capacity of layered clay. To investigate the difference in bearing capacity of suction anchors in layered clay and homogeneous clay under inclined loading, the same numerical model shown in Figure 1 was employed to analyze the pullout bearing capacity of suction anchors for different clay strengths S_{um}/kD (Clay A to Clay D) as listed in Table 1. The optimum centerline loading depth, uniaxial ultimate load capacity, and VH failure envelopes under corresponding operating conditions were investigated.

It can be seen from Figure 9 that for homogeneous clay with varying S_{um}/kD, as the clay strength increases, $Z_{cl,opt}$ decreases from 0.71 to 0.69. The increase in S_{um}/kD indicates a higher proportion of shear strength near the mud surface, shifting the center of gravity of the anchor shear strength upward. According to the principle of moment equilibrium, to prevent anchor rotation, $Z_{cl,opt}$ shifts slightly upward. Overall, $Z_{cl,opt}$ had little change.

 doi:10.20944/preprints202510.2499.v1

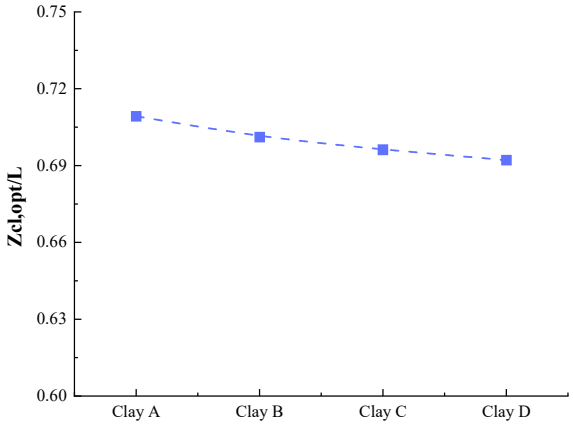

Figure 9. Optimal centerline loading depth Zcl,opt for suction anchors in homogeneous clay.

Compared with the results in Section 4.1, it can be observed that the homogeneous clay Zcl,opt is solely influenced by S_{um}/kD, which has a more stable variation pattern. For layered clays, $Z_{cl,opt}$ is primarily affected by the LOC layer, while the influence of the NC and LNC layers on Zcl,opt is masked by the high-strength LOC layer. This indicates that layered soils differ from homogeneous soils in their single correlation of 'S_{um}/kD-$Z_{cl,opt}$,' with the thickness of high-strength soil layers being the core variable controlling $Z_{cl,opt}$. By comparing the findings of Fu et al. [29] on homogeneous clay $Z_{cl,opt}$, the accuracy of the constructed numerical model can be further validated.

In combination with Figure 10, it can be observed that as S_{um}/kD increases, the uniaxial ultimate bearing capacity grows synchronously. However, the rate of increase varies: when S_{um}/kD rises from 0.4 to 1.0, the horizontal ultimate bearing capacity H_{ult} increases from 2915.65 kN to 5095.8 kN (an increase of approximately 74.8%), while the vertical ultimate bearing capacity V_{ult} increases from 3976.02 kN to 7317.5 kN (an increase of approximately 84.0%). The increase in H_{ult} is more pronounced. This difference stems from the distinct mechanisms governing bearing capacity. Horizontal bearing capacity relies on the uniform mobilization of lateral friction resistance throughout the entire anchor length; as S_{um}/kD increases, lateral friction resistance at all anchor depths rises synchronously. In contrast, vertical bearing capacity is simultaneously influenced by end resistance, this also results in a higher increment of vertical ultimate bearing capacity than that of horizontal ultimate bearing capacity.

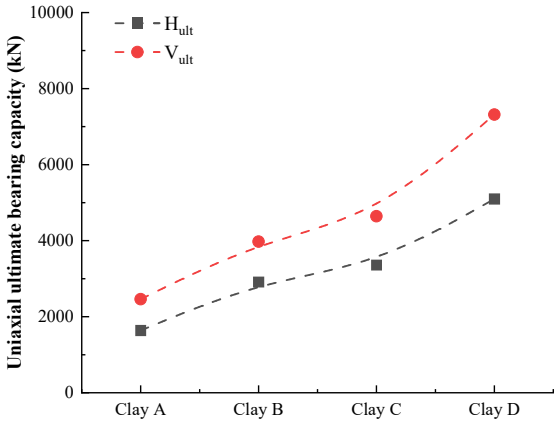

Figure 10. Uniaxial ultimate bearing capacity H_{ult} and V_{ult} for homogeneous clay.

In comparison with Section 4.2, it is evident that H_{ult} in layered clay is largely unaffected by the thicknesses of NC and LNC layers. When T_c/L increases from 0.5 to 1.25, H_{ult} remains nearly constant,

 doi:10.20944/preprints202510.2499.v1

being controlled solely by the LOC layer thickness T_h/L; whereas V_{ult} is influenced by both T_h/L and T_c/L. When T_c/L increases to 1.25, V_{ult} increases by approximately 35%. This contrasts with the behavior in homogeneous clay, where both H_{ult} and V_{ult} are governed by a single S_{um}/kD. Horizontal bearing capacity is more sensitive to the upper high-strength soil layer, while vertical bearing capacity is influenced by the coupled effects of multiple soil layers.

The VH failure envelopes for homogeneous clay are shown in Figure 11. By comparing with Section 4.3, it can be observed that the VH envelopes of layered clay exhibits distinct differences from that of homogeneous clay. Specifically, when horizontal bearing capacity is high, the envelope retains relatively high vertical bearing capacity, with the LOC layer providing significant lateral friction resistance. Conversely, when vertical bearing capacity is high, the envelope corresponds to a decrease in bearing capacity, where the anchor tip may be located in the NC or LNC layer, resulting in reduced end resistance.

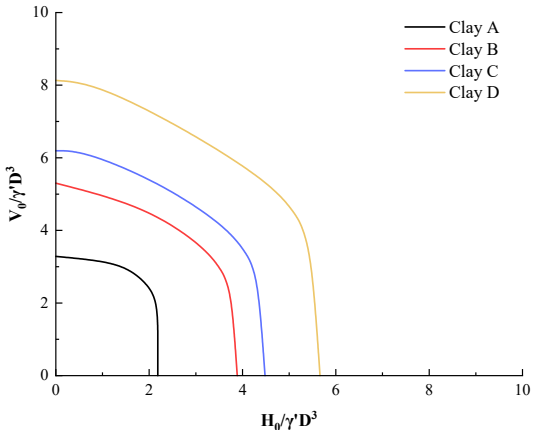

Figure 11. The VH failure envelopes for homogeneous clay.

A comprehensive analysis reveals significant differences in the pullout resistance of suction anchors in homogeneous clay and layered clay. While extensive research has focused on the bearing capacity of suction anchors in homogeneous clay, it is essential to investigate their pullout resistance in layered clay.

6. Limitations

This study conducted a series of pullout bearing capacity analyses for suction anchors with a commonly used L/D=1.5 in engineering applications, specifically within upper- stiff-lower-soft clay. It systematically investigated the effects of upper- stiff-lower-soft layered clay on the optimal centerline loading depth $Z_{cl,opt}$, uniaxial ultimate bearing capacity H_{ult} and V_{ult}, and VH failure envelopes of suction anchors. The findings provide theoretical basis and practical guidance for optimizing the design and safety assessment of suction anchor foundations in layered clay. However, certain limitations remain:

(1) This paper investigates the pullout bearing capacity of suction anchors subjected to inclined loads in layered clay with upper- stiff-lower-soft. In practical engineering, layered clay exhibits diverse characteristics such as upper- stiff-lower-soft, upper-soft-lower hard, soft-hard-soft, and hard-soft-hard etc. Therefore, based on existing research, a systematic investigation into the bearing capacity of suction anchors in layered clay is necessary.

(2) This paper investigates the pullout bearing capacity of suction anchors with a L/D =1.5 in layered clay. In practical engineering applications, the L/D of suction anchors varies according to project design (ranging from L/D=1 to 10). Therefore, further research is required to study the pullout bearing capacity in layered clay under a wide range of L/D.

 doi:10.20944/preprints202510.2499.v1

(3) This paper only systematically analyzes the pullout capacity of suction anchors and does not examine in detail how pullout capacity varies with different padeyes. Further research is needed to analyze the pullout capacity of suction anchors at different padeyes under inclined loads.

7. Conclusion

In this paper, finite element numerical simulations were conducted to investigate the pullout capacity of suction anchors under inclined loading. The study examined the effects of varying soil parameters S_{um}/kD and layer thickness ratios T_h/L and T_c/L on the optimum centerline loading depth $Z_{cl,opt}$, uniaxial ultimate bearing capacity (H_{ult} and V_{ult}), and VH failure envelope of suction anchors. The main conclusions are as follows.

(1) The layer thickness ratio Th/L of the LOC is the core factor controlling $Z_{cl,opt}$. When the suction anchor partially embeds into the LOC layer, as the LOC layer thickness increases, the upper portion of the suction anchor contributes more lateral friction resistance. To balance the moments, the suction anchors $Z_{cl,opt}$ shifts downward. When the suction anchor is fully embedded in the LOC soil layer, $Z_{cl,opt}$ depends solely on the parameters of the LOC soil mass.

(2) The thickness ratio T_h/L of the LOC soil layer is the core factor determining the uniaxial ultimate bearing capacity, as the undrained shear strength of the LOC layer is significantly higher than that of the NC layer.With the larger the length of the suction anchor embedded into the LOC layer, the combined effect of lateral friction resistance and end resistance at the anchor-soil interface becomes more pronounced. The layered soil makes the soil strength along the clay surface exhibit non-uniformity. The increase in S_{um}/kD enhances the uniaxial bearing capacity of layered clay. The thickness of the NC layer T_c/L, has little effect on the horizontal ultimate bearing capacity H_{ult} but significantly influences the vertical ultimate bearing capacity V_{ult}.

(3) The strength of the LOC soil is relatively high. As the thickness ratio T_h/L increases, the contact area between the suction anchor and the high-strength clay expands, which provides more uniform and greater lateral friction at the anchor-soil interface. When the horizontal bearing capacity increases, the decrease in vertical bearing capacity becomes more gradual. The lower bound solution for the VH failure envelope of the corresponding layered soil has been obtained.

(4) A comparative analysis of the pullout bearing capacity of suction anchors under inclined loads in layered clay and homogeneous clay reveals that soil layering significantly affects the bearing capacity of suction anchors. In homogeneous clay, the pullout bearing capacity of suction anchors is solely influenced by the soil strength S_{um}/kD. In contrast, the pullout bearing capacity in layered clay is affected by factors including the soil strength S_{um}/kD and the soil layer thickness ratio T/L.

Author Contributions: Conceptualization, C. J. and L. L.; Methodology, X. Z., H. W. and D. F.; Formal analysis, H. W. and L. L.; Investigation, C. J. and H. W.; Resources, X. Z. and D. F.; Writing—original draft, C. J. and H. W.; Writing—review & editing, X. Z., L. L. and D. F.; Visualization, H. W.; Supervision, L. L.; Project administration, X. Z.; Funding acquisition, L. L. and D. F. All authors have read and agreed to the published version of the manuscript.

Funding: The authors would like to acknowledge the consistent support provided by the National Natural Science Foundation of China (through the grant of No. 52394251), the Natural Science Foundation of Shandong Province (Grant ZR2022YQ54), and the Taishan Scholars Programs. Their support is gratefully acknowledged.

Institutional Review Board Statement: Not applicable.

Informed Consent Statement: Not applicable.

Data Availability Statement: Data will be made available on request.

Conflicts of Interest: Authors Cheng-Liang Ji and Xia-Tao Zhang are employed by the Shandong Electric Power Engineering Consulting Institute Corporation Limited. The remaining authors declare that the research was conducted in the absence of any commercial or financial relationships that could be construed as a potential conflict of interest.

 doi:10.20944/preprints202510.2499.v1

References

1. Tjelta, T. I. Suction Piles: Their Position and Application Today. **2001**.
2. Andersen, K.H.; Jostad, H.P. Foundation design of skirted foundations and anchors in clay. *InOffshore technology conference.* **1999,** OTC-10824. OTC.
3. Andersen, K.H.; Murff, J.D.; Randolph, M.F.; Clukey, E.C.; Erbrich, C.T.; Jostad, H.P.; Hansen, B.; Aubeny, C.; Sharma, P.; Supachawarote, C. Suction anchors for deepwater applications. InProceedings of the 1st international symposium on frontiers in offshore geotechnics, *ISFOG.* **2005,** 3-30.
4. Cheng, L.; Hossain, M.S.; Hu, Y.; Kim, Y.H.; Ullah, S.N. Failure envelope of suction caisson anchors subjected to combined loadings in sand. *Appl. Ocean. Res*. **2021,** 114:102801.
5. Mohiuddin, M.A.; Hossain, M.S.; Kim, Y.H.; Hu, Y.; Ullah, S.N. Insight into the Behavior of a Caisson Anchor under Cyclic Loading in Calcareous Silt. *J. Geotech. Geoenviron.* **2022,** 148, (7): 04022047.
6. Bhattacharjee, S.; Majhi, S.; Smith, D.; Garrity, R. Serpentina FPSO mooring integrity issues and system replacement: unique fast track approach. *InOffshore Technology Conference.* **2014,** D031S033R003. OTC.
7. Panayides, S.; Powell, T.A.; Schrøder, K. Penetration resistance of suction caissons in layered soils–A case study. *InOffshore Site Investigation Geotechnics 8th International Conference Proceeding.* **2017,** 562-569. Society for Underwater Technology.
8. Li, D.; Hou, X.; Zhang, Y. Shearing behavior of suction caisson wall-sand interface throughout the suction caisson life-cycle. *Appl. Ocean. Res*. **2024,** 142:103852.
9. Lei, G.; Wang, K.; Cheng, W.; Zhang, L. A Novel Analytical Model of Gas-Water Relative Permeability in Hydrate-Bearing Sediments Under Creep. *SPE Journal*. **2025,** 1:1-21.
10. Wang, J.H.; Liu. J.L.; Zhou, Y.R. Model tests on bearing capacities of suction anchors with taut mooring systems under combined static and cyclic loads. *Chin. J. Geotech. Eng*. **2012,** 34(6):997-1004.
11. El-Sherbiny, R.M. Performance of suction caisson anchors in normally consolidated clay. *The University of Texas at Austin*. **2006**.
12. Keaveny, J.M.; Hansen, S.B.; Madshus, C.; Dyvik, R. Horizontal capacity of large-scale model anchors. *InInternational conference on soil mechanics and foundation engineering.* **1994,** 677-680.
13. Newlin, J., Suction anchor piles for the Na Kika FDS mooring system part 1: Site characterization and design. *In Deepwater Mooring Systems: Concepts, Design, Analysis, and Materials*. **2003,** 28-54.
14. Wang, J.H.; Liu, J.L.; Chen, W.Q. Effects of Loading Direction on Ultimate Bearing Capacity of Suction Anchors With Taut Mooring System. *Chin. J. Geotech. Eng*. **2012,** 34(3):385-91.
15. Zhang, M.H.; Yin, Z.Y.; Fu, Y. Pull-out capacity and failure mechanism of suction anchors in clay considering trench configuration and local scour effects. *Eng. Geol*. **2025,** 347:107942.
16. Kim, S.; Choo, Y.W.; Kim, J.H.; Kim, D.S.; Kwon, O. Pullout resistance of group suction anchors in parallel array installed in silty sand subjected to horizontal loading–centrifuge and numerical modeling. *Ocean. Eng*. **2015**, 107:85-96.
17. Kim, S.R. Evaluation of vertical and horizontal bearing capacities of bucket foundations in clay. *Ocean. Eng*. **2012,** 52:75-82.
18. Zhou, M.; Yang, N.; Tian, Y.; Zhang, X. Inclined pullout capacity of suction anchors in clay over silty sand. *J. Geotech. Geoenviron*. **2023,** 149(6):04023030..
19. Zou, X.; Yang, Z.; Hu, J. Bearing capacity of monopile-bucket composite foundation in sand-over-clay under VHM combined static loads. *Appl. Ocean. Res*. **2024,** 150:104092.
20. Zhu, B.; Dai, J.L.; Kong, D.Q.; Feng L.Y, Chen Y.M. Centrifuge modelling of uplift response of suction caisson groups in soft clay. *Can. Geotech. J*. **2020,** 57(9):1294-303.
21. Subramaniam, R.; Banerjee, S. Three-Dimensional Numerical Analysis of Static and Cyclic Pull-out Response of Plate Anchors in Reinforced Soft Clay. *Int. J. Geosynth. Groun*. **2024,** 10(3):46.
22. Colliat, J.L.; Dendani, H.; Puech, A.; Nauroy, J.F. Gulf of Guinea deepwater sediments: Geotechnical properties, design issues and installation experiences. *InProceedings of the 2nd International Symposium on Frontiers in Offshore Geotechnics (ISFOG)*, Perth, Australia. **2011,** 59-86.
23. Lieng, J.T.; Tjelta, T.I.; Skaugset, K. Installation of two prototype deep penetrating anchors at the Gjoa Field in the North Sea. *InOffshore Technology Conference.* **2010,** OTC-20758. OTC.
24. Ehlers, C.; Chen, J.; Roberts, H.; Lee, Y. The origin of near-seafloor" crust zones" in deepwater. **2005**, 927.

 doi:10.20944/preprints202510.2499.v1

25. Chao, Z.; Wang, H.; Hu, S.; Wang, M.; Xu, S.; Zhang, W. Permeability and porosity of light-weight concrete with plastic waste aggregate: Experimental study and machine learning modelling. *Constr. Build. Mater*. **2024**, 411:134465.
26. Nissen. Geotechnical And Foundation Design Considerations. **2011**.
27. Bhattacharya, S. Design of foundations for offshore wind turbines. *John Wiley & Sons*. **2019.**
28. Kim, S.; Choo, Y.W.; Kim, D.S. Pullout capacity of horizontally loaded suction anchor installed in silty sand. *Mar. Georesources. Geotec.* **2016,** 34(1):87-95.
29. Fu, D.; Zhang, Y.; Yan, Y.; Jostad, H.P. Effects of tension gap on the holding capacity of suction anchors. *Mar. Struct.* 2**020**, 69:102679.
30. Houlsby, G.T.; Byrne, B.W. Design procedures for installation of suction caissons in clay and other materials. *Proceedings of the Institution of Civil Engineers-Geotechnical Engineering*. **2005,** 158(2):75-82.
31. Mi, Y.; Ma, H.; Yi, E.; Sun, K. Extraction of suction anchors in sand with overpressure-Experimental study and numerical analysis. *Ocean. Eng*. **2024,** 297:117058.
32. Supachawarote, C. Inclined load capacity of suction caisson in clay. *Perth: University of Western Australia*. **2006.**
33. Zhang, Y.; Andersen, K.H.; Tedesco, G. Ultimate bearing capacity of laterally loaded piles in clay–Some practical considerations. *Mar. Struct*. **2016,** 50:260-75.
34. Jia, N.; Zhang, P.; Liu, Y.; Ding, H. Bearing capacity of composite bucket foundations for offshore wind turbines in silty sand. *Ocean. Eng*. **2018,** 151:1-1.
35. Wang, X.; Tian, Y.; Li ,S.; Li. J. Exploring the bearing characteristics of suction bucket foundations in Offshore wind turbines: A comprehensive analysis of tensile and compressive behavior. *Ocean. Eng*. **2024,** 298:117234.
36. Davis, E.H.; Booker. J.R. The effect of increasing strength with depth on the bearing capacity of clays. *Geotechnique*. **1973,** 23(4):551-63.
37. Menzies, D.; Roper, R. Comparison of jackup rig spudcan penetration methods in clay. *InOffshore Technology Conference*. **2008,** OTC-19545. OTC.
38. Hung, L.C.; Kim, S.R. Evaluation of undrained bearing capacities of bucket foundations under combined loads. *Mar. Georesources. Geotec.* **2014,** 32(1):76-92.
39. Ma, H.L.; Feng, X.L.; Liu, L.L.; Zhang, A.; Wang, D. Changes in the effective absolute permeability of hydrate-bearing sands during isotropic loading and unloading. *Petrol.m Sci.* **2025.**
40. Park, J.S.; Park. D. Vertical bearing capacity of bucket foundation in sand overlying clay. *Ocean. Eng*. **2017,** 134:62-76.
41. Wang, X.; Li, D.; Li, J. Centrifuge modeling and numerical analysis on lateral performance of mono-bucket foundation for offshore wind turbines. *Ocean. Engg*. **2022,** 259:111925.
42. Liu, R.; Meng, X.; Li, C.; Ma, W.; Chen, G. Suction penetration characteristics and resistance calculation of bucket foundation in sand. *Appl. Ocean. Res*. **2022,** 127:103300.
43. Long, C.; Liang, R.; Zhou, M.; Li, J.; Zhang, X. Inclined pullout capacity of suction anchors in clay-silty sand-clay soil deposits. *Appl. Ocean. Res*. **2025,** 158:104549.
44. Zhao, L.; Gaudin, C.; O'loughlin, C.D.; Hambleton, J.P.; Cassidy, M.J.; Herduin, M. Drained capacity of a suction caisson in sand under inclined loading. *J. Geotech. Geoenviron*. **2019,** 145(2):04018107.
45. Gourvenec, S. Effect of embedment on the undrained capacity of shallow foundations under general loading. *Geotechnique*. **2008,** 58(3):177-85.
46. Gourvenec, S.; Randolph, M. Effect of strength non-homogeneity on the shape of failure envelopes for combined loading of strip and circular foundations on clay. *Geotechnique*. **2003**, 53(6):575-86.